DETECTION AND MAPPING OF MINERALIZED AREAS IN THE CORTEZ-UINTA BELT, UTAH-NEVADA, USING COMPUTER-ENHANCED ERTS IMAGERY

TYPE II PROGRESS REPORT

Original photography may be purchased from:
EROS Data Center
10th and Dakota Avenue
Sioux Falls, SD 57198

ORIGINAL CONTAINS
COLOR ILLUSTRATIONS

Submitted by:

Lawrence C. Rowan
Principal Investigator
U. S. Geological Survey
National Center, Stop 927
Reston, Virginia 22092

15 February 1976

C. Significant Results.

Mineralogical differences between hydrothermally altered rocks and most unaltered rocks in south-central Nevada cause visible and near-infrared (0.45-2.4 μm) spectral reflectance differences which can be used to discriminate these broad categories of rocks in multispectral images. The most important mineralogical differences are the increased abundance of goethite, hematite, jarosite, alunite, montmorillonite, and kaolinite in the altered zones. Analysis of reflectance spectra recorded in the field showed that the altered rock spectra are characterized by broad absorption bands in the 0.45-0.50 μm and 0.85-0.95 μm regions, which are due to electronic processes in the iron ions, and an absorption band near 2.2 μm, which is due to vibrational processes in the hydroxyl ions. These features are absent or weak in most of the unaltered rock spectra. Therefore, the shapes of the 0.45-2.4 μm spectra for these altered and unaltered rocks are conspicuously different.

However, because of the wavelength positions and widths of the Landsat Multispectral Scanner (MSS) bands, these spectral differences are not apparent in individual or color-infrared composite MSS images. The technique developed to enhance these subtle spectral differences combines ratioing of the MSS bands and contrast stretching. The stretched-ratio values are used to produce black-and-white images that depict materials according to spectral reflectance; ratioing minimizes the influence of topography and overall albedo on the grouping of spectrally similar materials. Color compositing of two or more stretched-ratio images to form color-ratio

composites provides additional enhancement. The most effective color-ratio composite for discriminating between the altered and unaltered areas, as well as among many of the unaltered rocks in south-central Nevada, was prepared using the following diazo color and stretched-ratio image combinations: blue for MSS 4/5, yellow for MSS 5/6, and magenta for MSS 6/7. Altered areas appear green and brown in this combination.

Field evaluation of this color-ratio composite shows that, after exclusion of alluvial areas, approximately 80% of the green and brown color patterns are related to hydrothermal alteration. The remaining 20% consists mainly of pink hematitic crystallized tuff and tan or red ferruginous shale and siltstone. Discrimination of this unaltered tuff from the altered rocks may be possible in the 2.2 μm region because this absorption band is absent in the tuff spectra. However, the shale and siltstone are mineralogically and spectrally similar to the altered rocks; hence, there appears to be little prospect of distinguishing these rocks in visible and near-infrared multispectral images.

NOTE: See attached document.

D. Publications.

Rowan, Lawrence,C., Goetz, Alexander F.H., and Ashley, Roger P., 1975, Machine Processing of Landsat (ERTS) Data in the Search for Alteration Halos [abst.], in Proceedings of the Pecora Symposium, 28-31 Oct 75, Sioux Falls, S.D.

Rowan, Lawrence C., Goetz, Alexander F.H., and Ashley, Roger P., 1975, Detection and Mapping of Hydrothermal Alteration Zones in South-Central Nevada by Use of Computer-Enhanced Landsat Images [abst.], in Abstracts of Keynote Addresses and Short Communications, Meeting of European Geological Societies, Reading University, UK, 8-12 Sep 75.

Rowan, Lawrence C., Goetz, Alexander F.H., Ashley, Roger P., and Seigal, Barry S., 1975, Discrimination of Hydrothermally Altered and Unaltered Rocks in Visible and Near-Infrared Multispectral Images [abst.], in Proceedings of the Annual Meeting of the Society of Exploration Geophysics, 6-8 Oct 75 Denver, Co.

Goetz, Alexander F.H., Rowan, Lawrence C., and Seigal, Barry S., 1975, Quantitative Spectral Techniques and Computer Image Processing as Applied to Lithologic Mapping [abst.], in Proceedings of the IEEE Meeting, Houston, Texas, 12 Dec 75.

Rowan, Lawrence C., Goetz, Alexander F.H., Ashley, Roger P., and Seigal, Barry S., in press, Discrimination of Hydrothermally Altered and Unaltered Rocks in Visible and Near-Infrared Multispectral Images, submitted to Society of Exploration Geophysics.

E. Recommendations.

None.

F. Funds Expended.

Total expenditures - $41,792.57.

G. Data Use.

	Value of Data Allowed (U.S. Dollars)	Value of Data Ordered (U.S. Dollars)	Value of Data Received (U.S. Dollars)
Images	2600	2755	2755
Photos	11540	1370	1370
CCTs	400	400	400

H. Aircraft Data.

In spite of the delay in delivery of aircraft data, the color and color-infrared photographs continue to be an important data source, especially for estimating vegetation cover, locating sites for spectral measurements, and logistical purposes.

DISCRIMINATION OF HYDROTHERMALLY ALTERED AND UNALTERED ROCKS IN VISIBLE AND NEAR INFRARED MULTISPECTRAL IMAGES

by

Lawrence C. Rowan, U. S. Geological Survey, Reston, Va.
Alexander F. H. Goetz, Jet Propulsion Laboratory, Pasadena, Calif.
Roger P. Ashley, U. S. Geological Survey, Menlo Park, Calif.

Publication authorized by the Director, U. S. Geological Survey

Contents

	Page
Abstract	i
Introduction	1
Spectral Reflectance Studies	3
Goldfield Mining District	3
Reflectance Spectra	6
Image Analysis	10
Conclusions	21
References Cited	23

Illustrations

		Page
Figure 1.	ERTS-1 image mosaic showing locations of two study areas	2a
Figure 2.	*In situ* reflectance spectra for altered and unaltered rocks in the Goldfield, Nevada mining district.	7a-c
Figure 3.	*In situ* reflectance spectra for tan and red shales and pink hematitic tuff	9a
Figure 4.	*In situ* reflectance spectra over the MSS response range for altered and unaltered rocks in the Goldfield, Nevada mining district	9b
Figure 5.	Simplified two dimensional radiation geometry diagram	13a
Figure 6.	Path radiance-induced MSS 4/5 ratio error as a function of average spectral reflectance.	13a
Figure 7.	Color-ratio composite of MSS scene E1072-18001	16b
Figure 8.	Skylab S190A color photograph of part of the study area.	18a

Tables

	Page
Table 1. Composite description of field spectra sample sites in the Goldfield, Nevada mining district	7d, e
Table 2. MSS reflectance calculated from altered and unaltered rock spectra	9c
Table 3. MSS ratios for altered and unaltered rocks in the Goldfield, Nevada mining district.	16a

U. S. GOVERNMENT PRINTING OFFICE: 1978 O - 677-544

Discrimination of Hydrothermally Altered and Unaltered Rocks in Visible and Near Infrared Multispectral Images

by

Lawrence C. Rowan, U.S. Geological Survey, Reston, Va.
Alexander F.H. Goetz, Jet Propulsion Laboratory, Pasadena, Ca.
Roger P. Ashley, U.S. Geological Survey, Menlo Park, Ca.

Abstract

Mineralogical differences between altered rocks and most unaltered rocks in south-central Nevada cause visible and near-infrared (0.45 to 2.4 μm) spectral-reflectance differences which can be used to discriminate these broad categories of rocks in multispectral images. The most important mineralogical differences are the increased abundance of goethite, hematite, and jarosite, and the presence of alunite, montmorillonite, and kaolinite in the altered rocks. Analysis of reflectance spectra recorded in the field showed that the altered rock spectra are characterized by broad absorption bands in the 0.45-0.50 μm and 0.85-0.95 μm regions which are due to electronic processes in the iron ions, and a band near 2.2 μm which is due to vibrational processes in the OH ions. These features are absent or weak in most of the unaltered rock spectra. Therefore, the shapes of the 0.45-2.4 μm spectra for these altered and unaltered rocks are conspicuously different. However, because of the wavelength positions and widths of the Landsat Multispectral Scanner (MSS) bands, these spectral differences are not apparent in individual or color-infrared composite MSS images.

The technique developed to enhance these subtle spectral differences combines ratioing of the MSS bands and contrast stretching. The stretched ratio values are used to produce black-and-white images which depict materials according to spectral reflectance; ratioing minimizes the influence of topography and overall albedo on the grouping of spectrally similar materials. Color compositing of two or more stretched ratio images to form color-ratio composites provides additional enhancement. The most effective color-ratio composite for discriminating between the altered and unaltered areas, as well as among many of the unaltered rocks in south-central Nevada, was prepared using the following diazo color and stretched ratio image combinations: blue for MSS 4/5, yellow for MSS 5/6, and magenta for MSS 6/7. Altered areas appear green and brown in this combination.

Field evaluation of this color-ratio composite shows that excluding alluvial areas, approximately 80 percent of the green and brown color patterns are related to hydrothermal alteration. The remaining 20 percent consists mainly of pink hematitic crystallized tuff, a result of vapor-phase crystallization, and of tan and red ferruginous shale and siltstone. Discrimination of this unaltered tuff from the altered rocks may be possible in the 2.2 μm region because this absorption band is absent in the tuff spectra. However, because the shale and siltstone are mineralogically and spectrally similar to the altered rocks, there appears to be little prospect of distinguishing these rocks from altered rocks in visible and near-infrared multispectral images.

Introduction

Several workers have shown that exposed hydrothermally altered areas can be detected and mapped by analyzing the spectral radiance data recorded by the Landsat Multispectral Scanner (MSS) (Rowan and others, 1973; 1974; 1975 a, b; Schmidt, 1975; Schmidt and others, 1975; Albert, 1975; Goetz, 1975, written communication). Effective use of this technique must take into account a large number of variables, including the mineralogy of the altered and unaltered rocks, vegetation type and distribution, surface coatings, atmospheric scattering and transmission, solar illumination angles, soil moisture content, and grain size. The relationship between surface composition and spectral reflectance is fundamental and must be established before other factors can be evaluated.

This paper describes the initial results of a long-term study in which *in situ* measurements of visible and near-infrared spectral reflectance analyses are being used in an effort to define the relationship between surface composition and spectral reflectance for a variety of alteration types. Although measurements obtained thus far are not sufficient for a detailed quantitative analysis, they show the principal spectral differences which constitute the basis of the technique developed by Rowan and others (1974) for discriminating between hydrothermally altered and unaltered rocks in the eastern part of MSS scene E1072-18001 of south-central Nevada (fig. 1). Since that initial study, the entire area covered by this scene (fig. 1) has been processed and most of it has been evaluated. The most important results of this evaluation are also presented here with emphasis on the problems encountered and on methods for solving some of the problems.

Figure 1 near here

The main value of this new approach to mineral exploration is that it augments traditional exploration methods by providing a rapid, practical means for compiling reconnaissance alterations maps of large arid and semi-arid regions. In addition, with the use of high spatial resolution systems, this technique may prove useful for mapping some mineralogically distinct zones within hydrothermally altered areas.

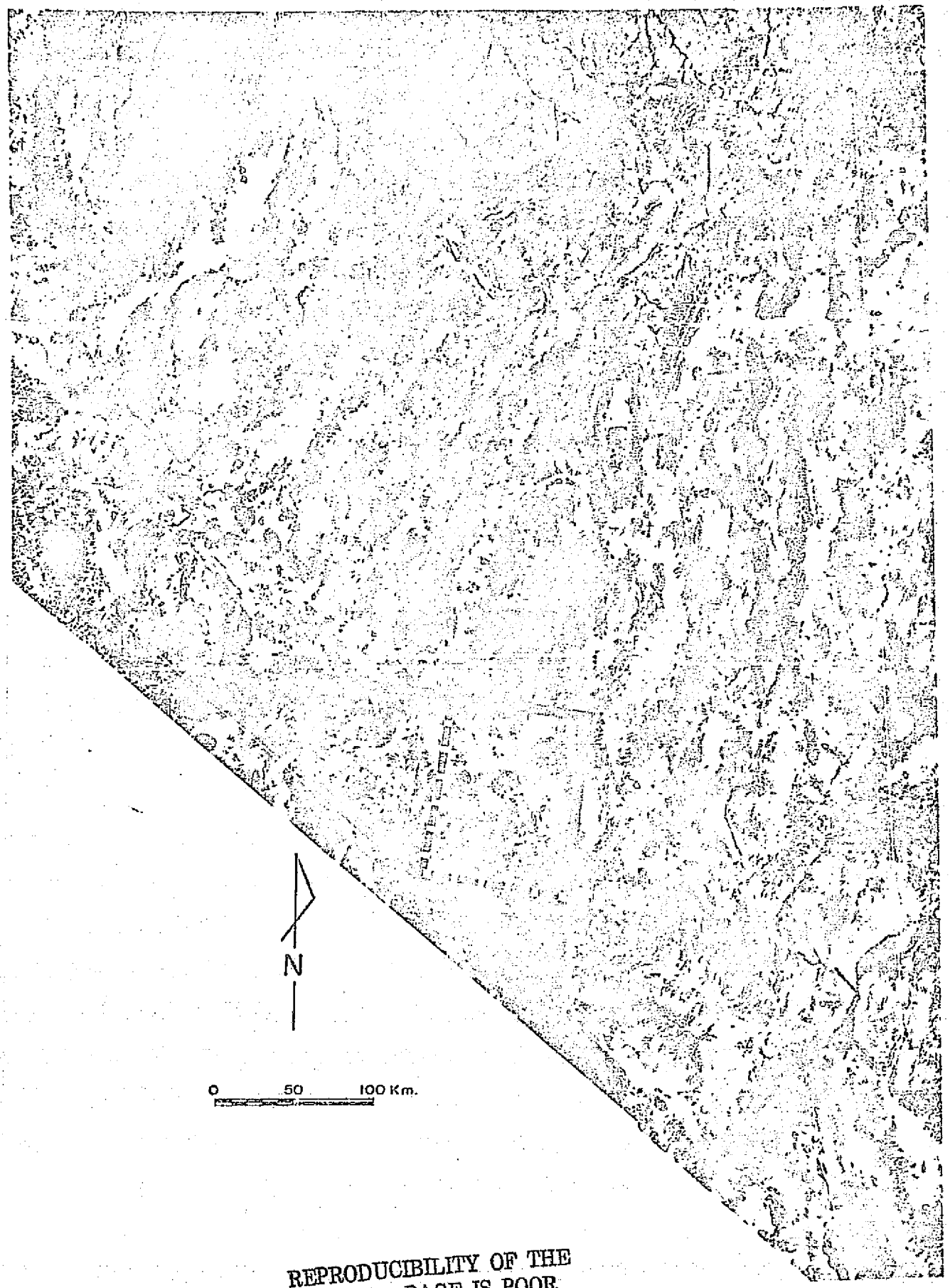

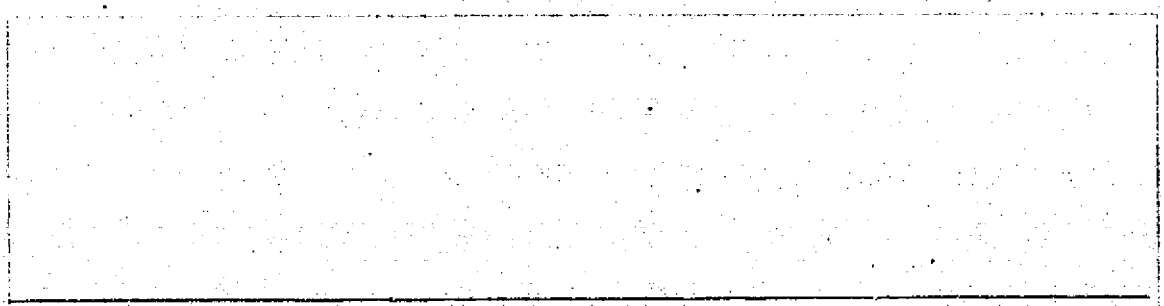

Figure 1. ERTS-1 image mosaic of Nevada showing location of the south-central Nevada study area. Dashed line shows approximate location of the initial study area described by Rowan and others (1974). GS locates central part of the Goldfield mining district.

Acknowledgments

We wish to thank Barry Seigal, Jet Propulsion Laboratory, Pasadena, California for his effort in the reduction of field spectrometer data and for his ideas on statistical analysis and representation of these data. We are also indebted to Dennis O'Leary and Howard Pohn of the U.S. Geological Survey, Denver, Colorado for many useful suggestions made in review of the manuscript.

This work was carried out jointly by the U.S. Geological Survey and the Jet Propulsion Laboratory, California Institute of Technology for the National Aeronautics and Space Administration under contracts S-53953-A and NAS 7-100, respectively.

Spectral Reflectance Studies

Goldfield Mining District.

Spectral reflectance studies have been concentrated thus far in the Goldfield, Nevada mining district (fig. 1) because of the wide range of representative altered rocks present. Exposures here are excellent; vegetation covers less than an estimated 10 percent of the ground and is reasonably uniform, except for a higher density in drainage channels. The geology of the district has been described in detail (Ransome, 1909, 1910 a, b; Locke, 1912 a, b; Searls, 1948; Albers and Kleinhampl, 1970; Ashley, 1970; Albers and Stewart, 1972; Cornwall, 1972; Ashley and Keith, 1973; Ashley and Albers, 1975). The Goldfield district is an area of mainly lower Miocene volcanic rocks overlying Ordovician shale and chert and Mesozoic granitic rocks. The Miocene units include trachyandesite, rhyodacite, quartz latite, and rhyolite tuff and flows. Middle Miocene or lower Pliocene basalt and welded tuff locally cap these units. Alteration is extensive, especially in the lower Miocene trachyandesite and rhyodacite, the main ore-bearing rocks.

Rock alteration at Goldfield is of two general types: hydrothermal and propylitic. Hydrothermal alteration is more intense and conspicuous and is economically more important because of its direct association with metallization in the district. Two main zones of hydrothermal alteration, silicic and argillic, can be recognized in the field by their topographic expressions and colors (Ashley, 1970, 1971). The silicified zones consist of crudely tabular bodies composed mainly of microcrystalline quartz and lesser amounts of alunite and kaolinite. These bodies form craggy resistant outcrops which commonly have numerous fractures coated with black or dark red hematite or goethite. Where this coating is absent, the white to gray color of the fresh rock is apparent. These bodies appear to have formed along faults, fractures, and locally permeable beds and represent the sites of highest temperatures and the most intense cation leaching during hydrothermal alteration.

The silicified bodies are surrounded by extensive zones of argillized rocks which have a bleached appearance due to destruction of ferromagnesian and calcic minerals by the hydrothermal fluids, and formation of such minerals as quartz, kaolinite, pyrophyllite, K-mica, and montmorillonite. Three subzones within the argillized zone have been recognized on the basis of mineralogical differences. In order of decreasing intensity of alteration, these are advanced argillic rocks with quartz, alunite and kaolinite; kaolinite - , K-mica-bearing argillic rocks; and montmorillonite-bearing rocks. The color of the argillic rocks ranges from nearly white, gray, and various pastel shades of red, purple, brown, and yellow in the two kaolinitic subzones to dominantly yellow and brown in the montmorillonitic subzone. Exposures are poorer in the argillic zone than in the silicified zone because debris shed from the resistant ledges locally cover much of the adjacent less resistant argillic rocks. Distinction of the argillic subzones is further complicated by the need for X-ray and petrographic analysis to identify the diagnostic mineral assemblages. Consequently, detailed mapping of the hydrothermal alteration is not yet complete.

Propylitic alteration is less obvious than hydrothermal alteration because the chemical changes are smaller. In general, plagioclase is saussuritized, mafic minerals are hydrated, and opaque minerals are locally oxidized. Harvey and Vitaliano (1964) considered propylitic alteration in the Goldfield district to be the weakest grade of hydrothermal alteration. Ashley (1974) suggests, however, that the propylitization may be related to deuteric processes. This view is supported by the discontinuous distribution of the propylitic rocks and the dependence of the resulting mineral assemblages on the composition of the host rocks.

Reflectance Spectra.

Measurements of the 0.45-2.4 μm spectral reflectance were made in the field for the altered rocks and the main unaltered rock units using a portable spectrometer designed and fabricated at the Jet Propulsion Laboratory, Pasadena, California (Goetz and others, 1975). The sampling procedure was mainly guided by the need to obtain spectra which represent the individual rock units as viewed by the MSS. An additional consideration was the need to select better spectral bands for discriminating rock types, especially altered and unaltered rocks. Because of the low spatial resolution of this system (79m), sample sites included areas composed of colluvium as well as outcrops. Such sites were practically unavoidable in areas where argillic rocks were overlain and mixed with silicified debris. Each sample site, covering approximately 100 sq. cm was viewed vertically and all spectra were normalized to calibrated standards.

The spectra discussed below are averages calculated from groups of individual spectra representing local variants of the surface units. Statistical analyses of the average spectra have not been conducted because of the limited amount of data presently available. However, these spectra are undoubtedly more representative of the surface units than could be obtained by measuring even a large number of samples in the laboratory. A statistical analysis of a larger number of individual sample spectra is being prepared.

Average reflectance spectra for representative sites in the altered areas and for the unaltered rock units are shown in fig. 2a and 2b, respectively. Generalized composite descriptions of each site are given in Table 1. The general shapes of the average spectral curves for the three altered areas are similar (fig. 2a). The spectral features responsible for these shapes are an absorption band in the ultraviolet region (not shown in fig. 2a) and several minor bands in the visible region, a broad band near 0.90 μm, and a sharper band centered at about 2.2 μm. Maximum reflectance therefore occurs near 1.6 μm. All the absorption bands in the ultraviolet and visible are due to electronic processes in the constituent iron ions of such minerals as hematite, goethite, jarosite, and montmorillonite (Hunt and Salisbury, 1970; Hunt and others, 1971). The 2.2 μm feature is a combination band related to OH stretching and Al-O-H bending that takes place at longer wavelengths in alunite and clay minerals (Hunt and others, 1973).

Figure 2a and 2b near here

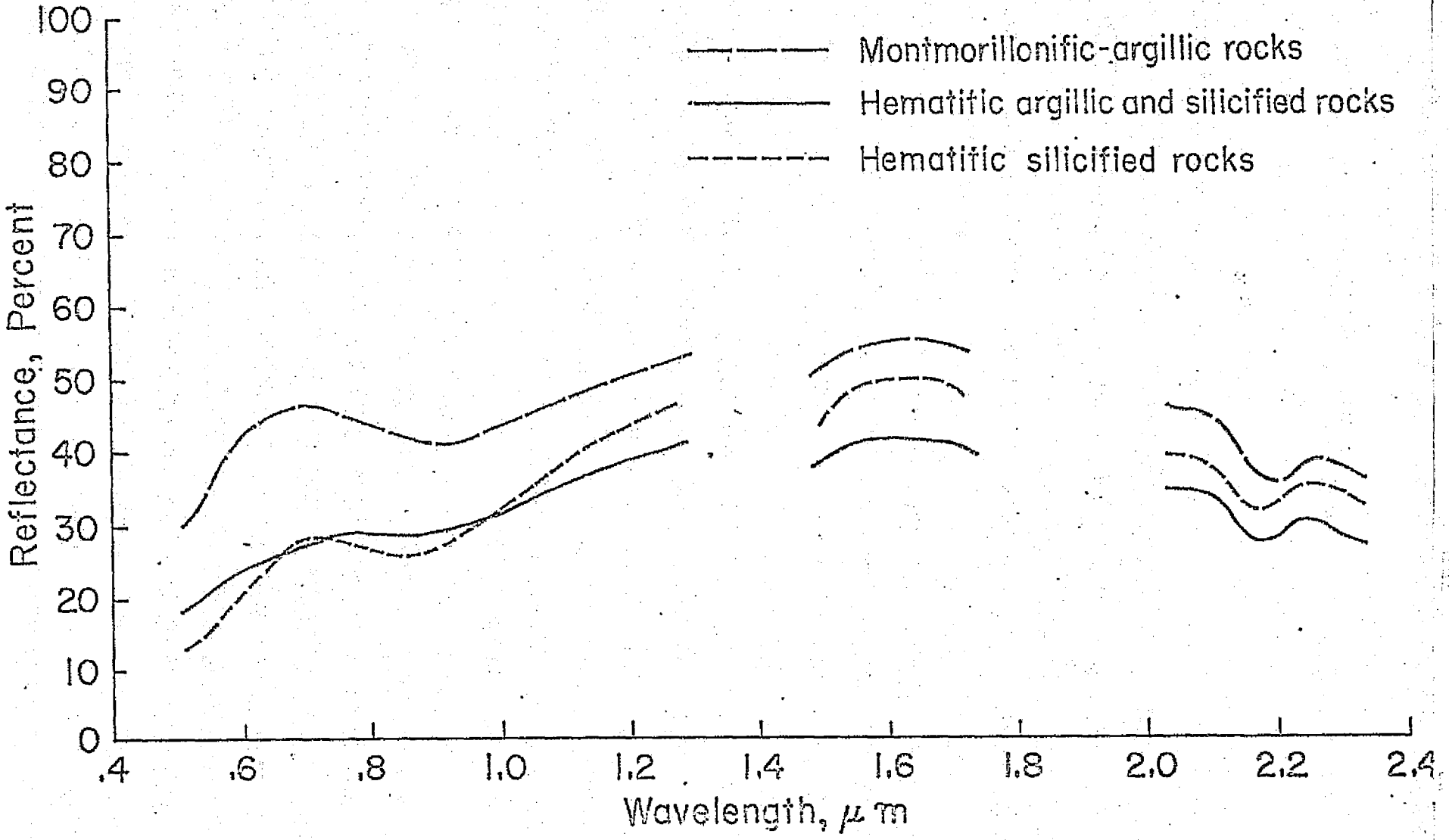
Montmorillonific-argillic rocks
Hematitic argillic and silicified rocks
Hematitic silicified rocks
Reflectance, Percent
100
90
80
70
60
50
40
30
20
10
0
.4
.6
.8
1.0
1.2
1.4
1.6
1.8
2.0
2.2
2.4
Wavelength, μm

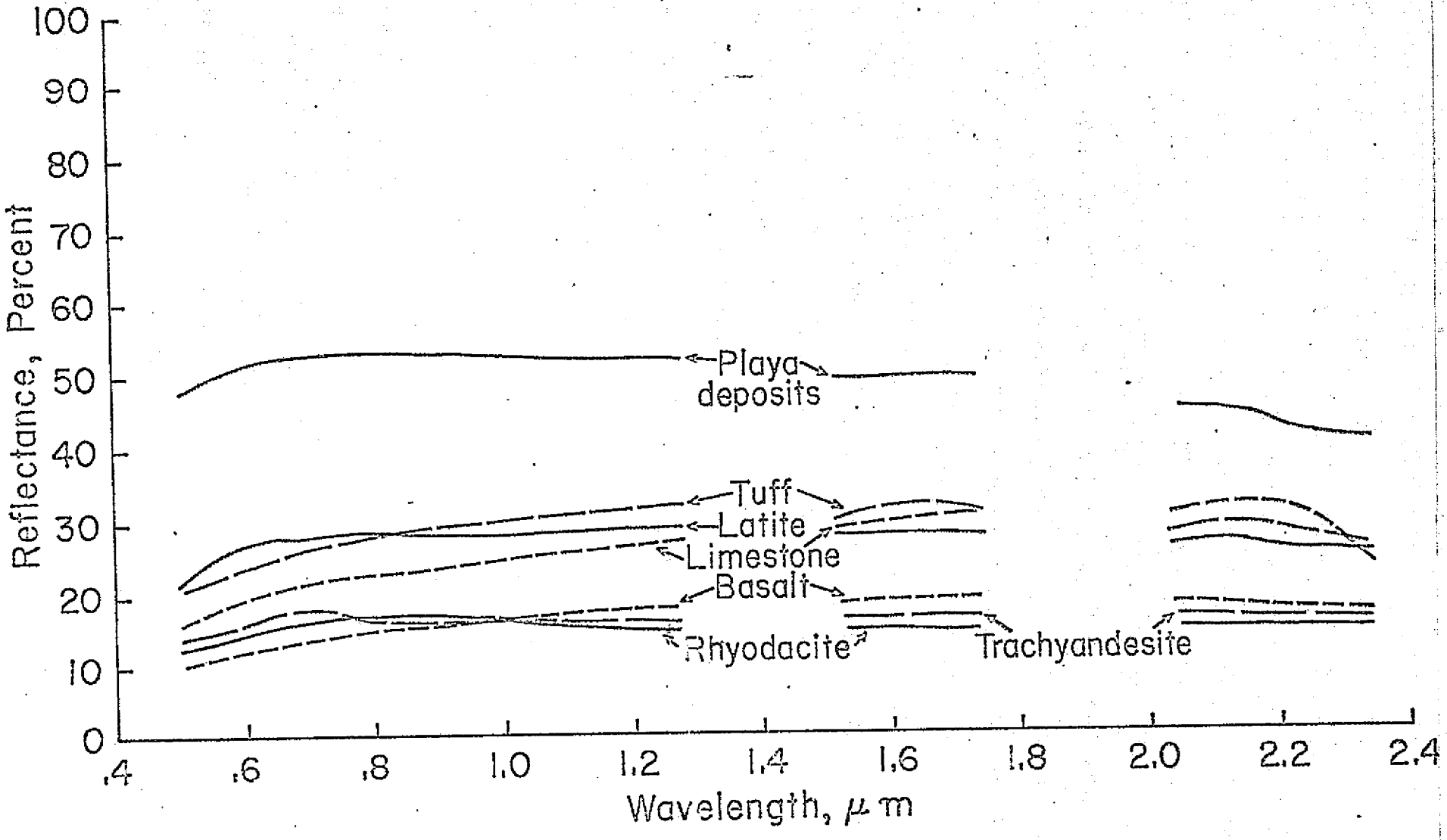
Reflectance, Percent
100
90
80
70
60
50
40
30
20
10
0
.4
.6
.8
1.0
1.2
1.4
1.6
1.8
2.0
2.2
2.4
Wavelength, μm
Playa deposits
Tuff
Latite
Limestone
Basalt
Rhyodacite
Trachyandesite

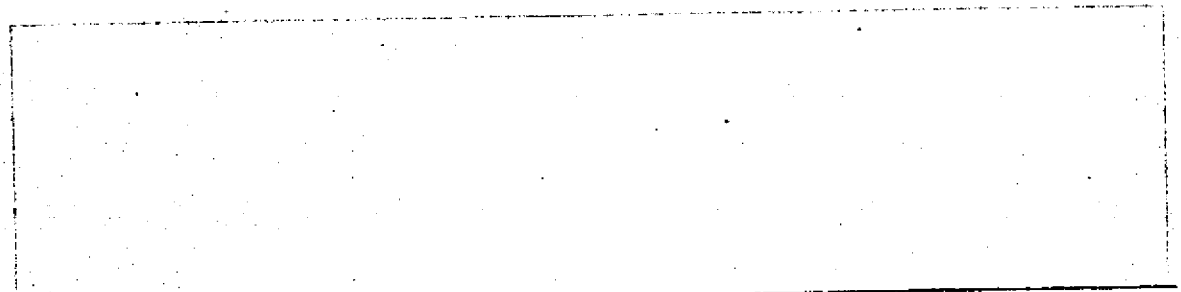

Figure 2. In situ reflectance spectra for (a) altered rock types and (b) unaltered rock types in and near the Goldfield, Nevada mining district. Areas of no data from about 1.3-1.5 μm and 1.7-2.0 μm are due to atmospheric absorption.

Table 1 - Generalized composite descriptions of selected sites within major altered and unaltered rock types in the Goldfield, Nev. mining district. 0.45-2.4 μm spectral reflectance measurements were recorded as well as the number of spectra for each rock unit.

Rock Type	Description	Number of Spectral Measurements
Hematitic Silicified Rocks	- Red, orange, yellow, black, and gray silicified fragments 0.5-10 across containing quartz, alunite, hematite, and jarosite; 5% to 20% tan, yellow, pink soil.	4
	Silicified outcrop with dark red and black hematite stain containing quartz, alunite, hematite, gypsum.	1
Hematitic argillic and Silicified Rocks	- Dark brown, black, orange, and red silicified fragments from 0.25-5 cm across containing quartz, kaolinite, alunite, and hematite; some pink, purple, gray, and white argillized fragments containing quartz, kaolinite, and hematite; 10% to 50% tan soil.	5
	- Black, tan, and red silicified outcrop containing quartz, alunite, and hematite.	3
Montmorillonitic Argillized Rocks	- Yellow brown, orange, purple, red, and white argillized fragments from 0.5 to 5 cm across containing quartz, kaolinite, alunite, jarosite, and hematite, montmorillonite, gypsum, and goethite; 5% to 90% yellow-tan soil.	5
Playa Deposits	- White, gray, and light tan containing quartz, feldspar, gypsum, calcite, illite (K-mica), and kaolinite.	25
Tuff	- Dark gray vitrophyric tuff outcrops.	5
	- Dark gray to tan vitrophyric tuff fragments from 0.5-5cm across; 5-20% tan silty soil.	2

Table 1 (continued)

Rock Unit	Description	Number of Spectra
Latite	Light gray, light brown, and orange propylitized quartz latite fragments from 0.25 to 4 cm across containing plagioclase, biotite, and hornblende, phenocrysts and ground mass containing plagioclase, glass and opaques; 15 to 20% tan silty soil.	3
Rhyodacite	Gray, blue-gray, dark brown, and dark red-brown porphyritic rhyodacite fragments from 0.5 to 6 cm across containing plagioclase, biotite, hornblende, hypersthene, and quartz phenocrysts, and ground mass of plagioclase, glass and alkali feldspar; 5-20% tan silty soil.	5
Trachyandesite	Medium gray pyroxene andesite fragments from 0.25 to 6 cm across containing plagioclase, augite, hypersthene, and hornblende phenocrysts and ground mass containing plagioclase, clino - and orthopyroxenes, and opaque minerals; 1% to 10% soil.	3
Basalt	Dark gray to black porphyritic basalt fragments from 0.5 to 5 cm across containing calcic plagioclase and olivine phenocrysts in ground mass of plagioclase microlites, augite, magnetite, glass, and biotite; 5 - 10% tan soil.	5
	Dark gray to black porphyritic basalt outcrops with same mineralogy as fragments.	4

Some of the small spectral differences reflect mineralogical differences among the altered areas. For example, the lower slope of the hematitic argillized and silicified rock spectrum in the visible region appears to be caused by less intense absorption bands due to the generally small amount of iron oxide minerals in this rock. Note also that the band near 0.90 μm occurs at a slightly longer wavelength in the montmorillonitic rocks (0.92 μm) than in the silicified rocks (0.87 μm). This difference is related to the presence of ferrous iron in montmorillonite (Hunt and Salisbury, 1970); in contrast, the other altered rocks contain dominantly ferric iron.

The average spectra for unaltered rocks (fig. 2b) in and near the Goldfield mining district display subtle differences in slope, but the iron and OH-absorption bands are absent or only weakly expressed. Consequently, these altered and unaltered rock spectra have conspicuously different shapes. Preliminary analysis of spectra obtained elsewhere in the study area indicates that these differences are representative of most of the other unaltered and altered rocks. However, two unaltered types are exceptional in this respect and a third is exceptional in the shorter wavelength part of the spectrum. Tan limonitic shale is widespread in the northwestern part of the area and red shale occurs locally in the southern part. Because the mineralogy of these rocks is similar to that of the altered rocks, their spectral shapes are nearly identical (figs. 2a and 3). The third rock type is an unusually bright pink crystallized tuff which is confined to the northern end of the Silver Peak Mountains south of Coaldale Junction, Nevada near the central part of the study area. The pink color of these rocks is attributed to the presence of numerous microscopic hematite particles in the groundmass formed during vapor-phase crystallization. Comparison of a representative in situ reflectance spectrum for the pink tuff and the altered rock spectra (figs. 4 and 2a, respectively) shows that they are similar between 0.45 and 1.8 μm, but the 2.2 μm absorption band characteristic of the altered rocks is not present in the tuff spectrum. The absence of this feature in the tuff spectrum is due to the general lack of hydrous phases in the tuff outcrops and in the residual soil, which is a product of mechanical rather than chemical weathering.

Figure 3 and 4 near here

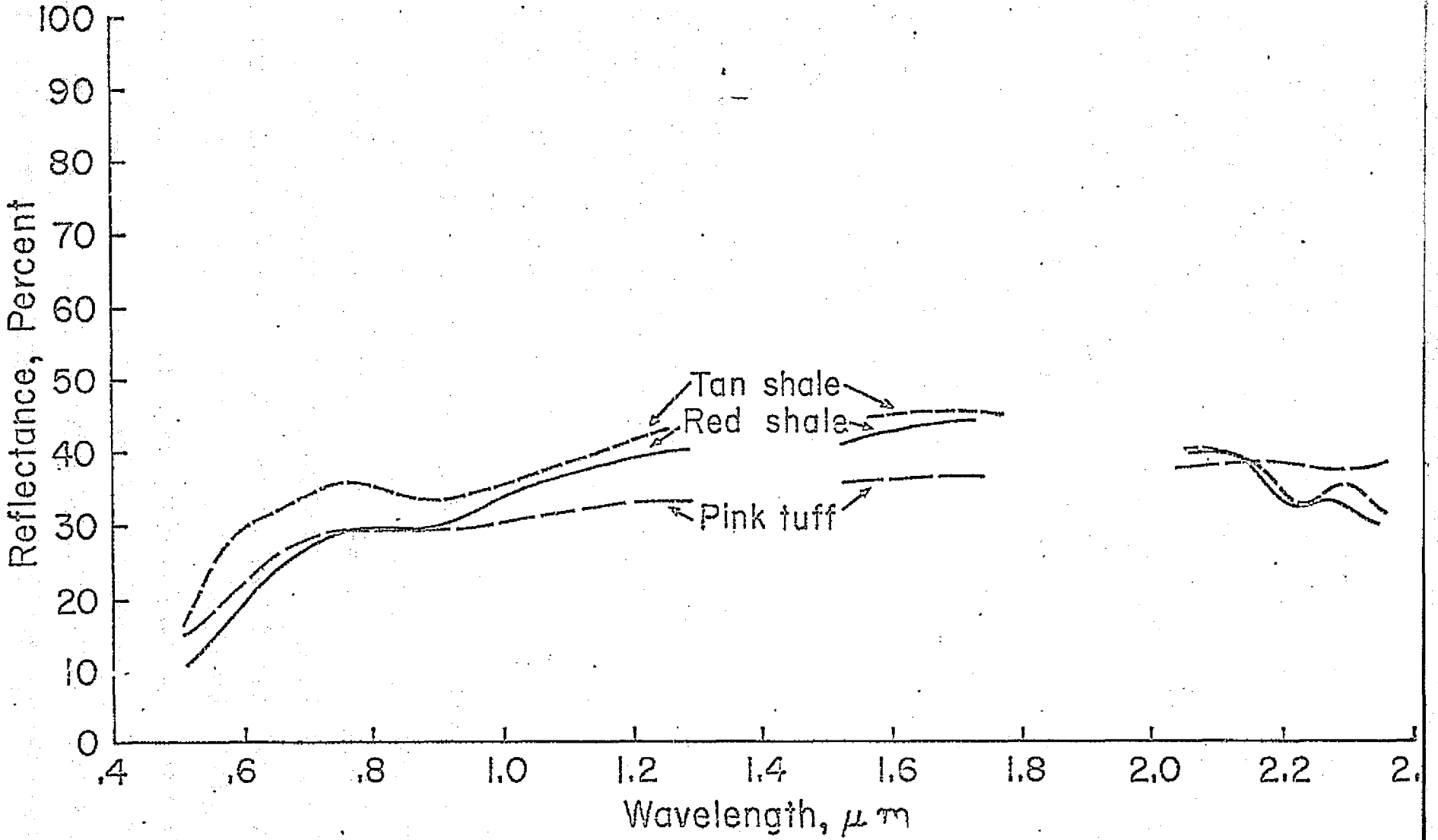
100
90
80
70
60
50
40
30
20
10
0
Reflectance, Percent
Tan shale
Red shale
Pink tuff
.4
.6
.8
1.0
1.2
1.4
1.6
1.8
2.0
2.2
2.
Wavelength, μm

Figure 3. In situ reflectance spectra for tan and red shales and tuff in the western part of MSS scene E1072-18001. Areas of no data from about 1.3-1.5 μm and 1.7-2.0 μm are due to atmospheric absorption.

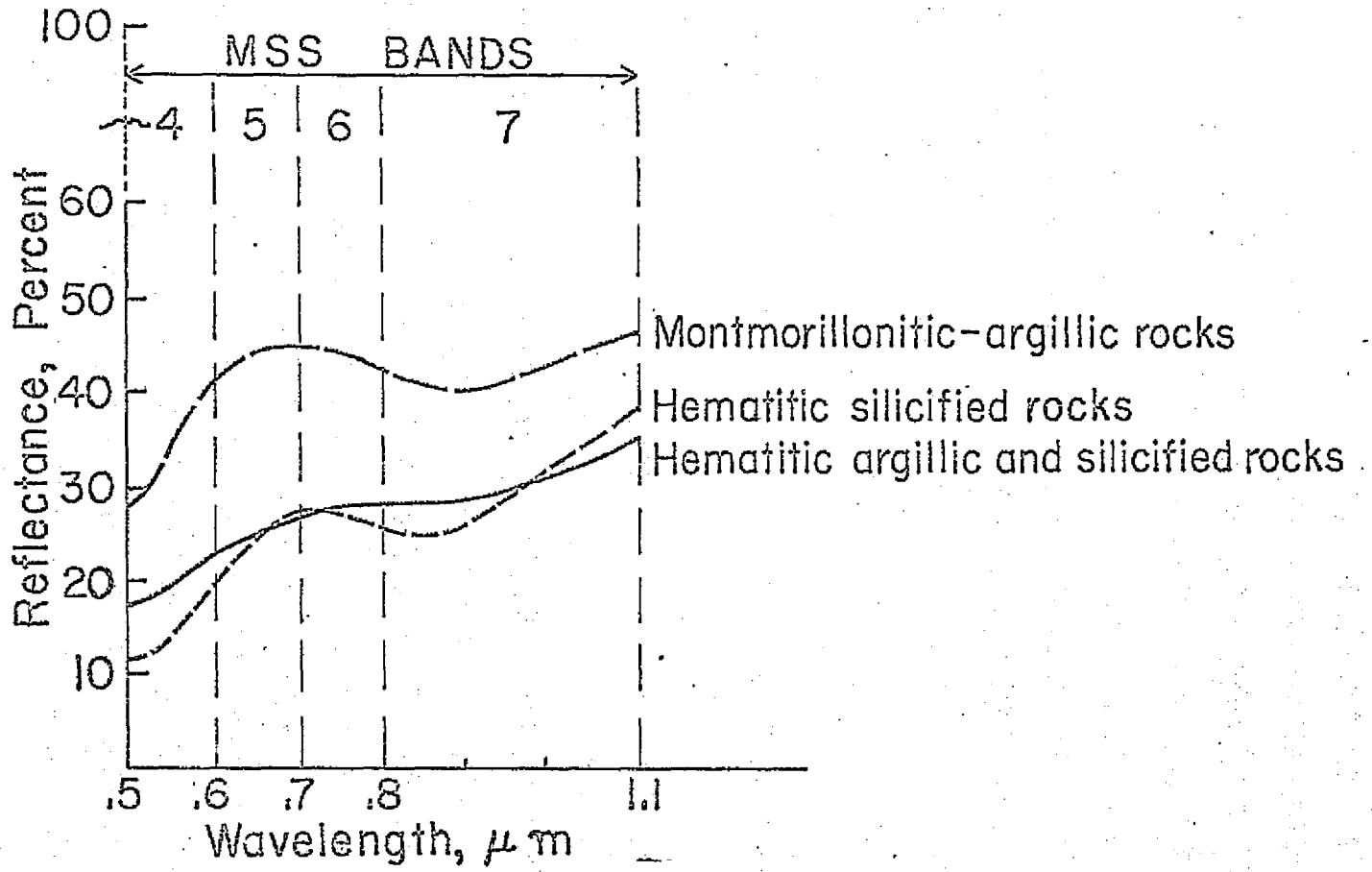

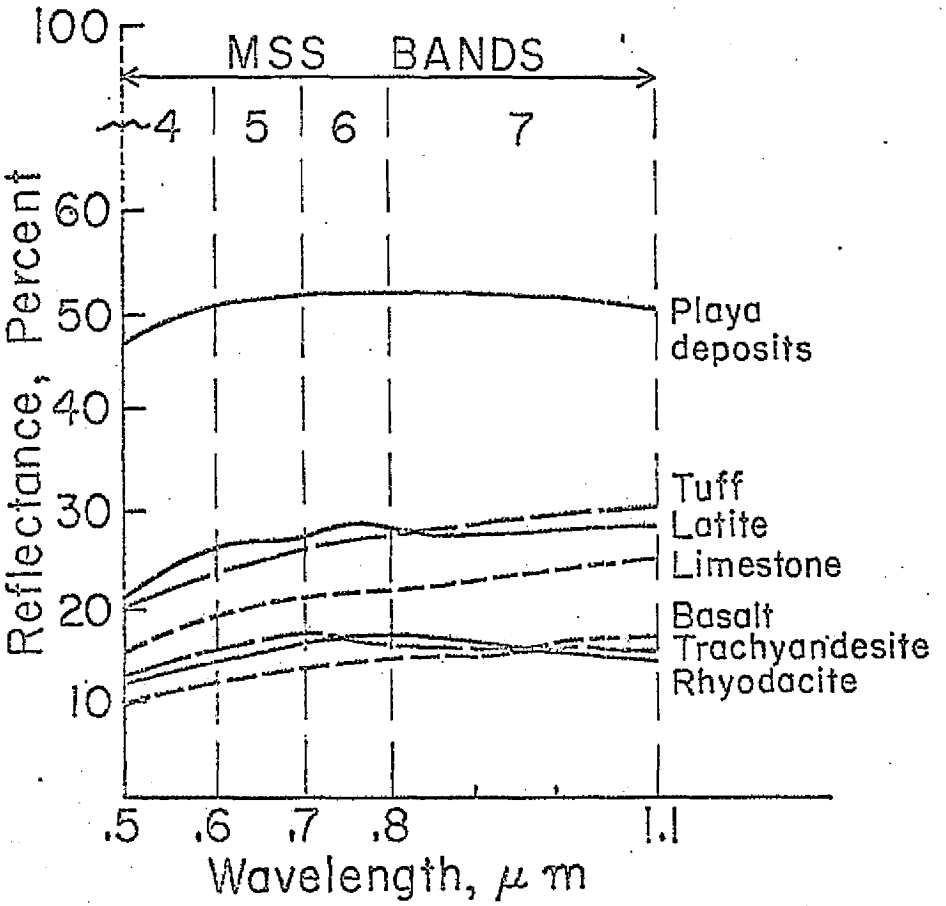
100
MSS BANDS
4
5
6
7
60
50
40
30
20
10
Reflectance, Percent
Playa deposits
Tuff
Latite
Limestone
Basalt
Trachyandesite
Rhyodacite
.5
.6
.7
.8
1.1
Wavelength, μm

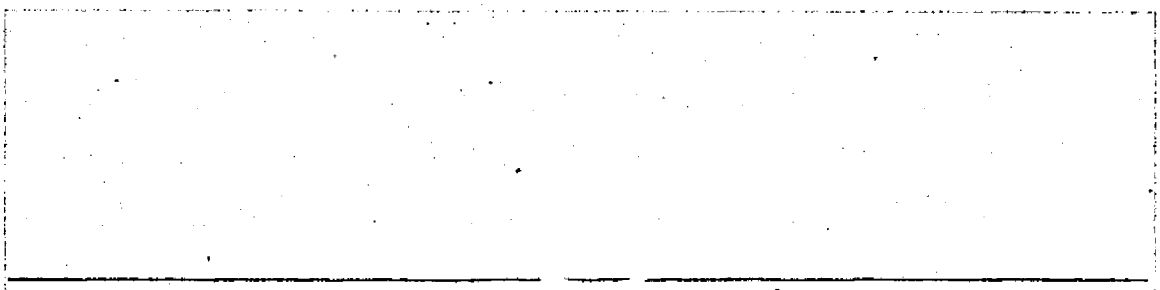

Figure 4. In situ reflectance spectra over the MSS response range for (a) altered rocks and (b) unaltered rocks in and near the Goldfield, Nevada mining district. Wavelength positions of the MSS bands are indicated.

Table 2

MSS reflectance in percent calculated for altered and unaltered rock spectra shown in fig. 3a and 3b, respectively.

MSS bands	Altered Rocks			Unaltered Rocks					
	Hematitic silicified	Hematitic argillic silicified	Montmorillonitic argillized	Playa deposits	Tuff	Latite	Rhyodacite	Trachyandesite	Basalt
4	13.5	20.9	35.0	49.3	15.7	22.8	12.1	12.7	9.6
5	23.0	25.9	42.4	51.2	19.4	26.1	13.8	14.8	11.5
6	26.4	28.9	42.5	52.3	21.7	26.6	14.5	15.0	12.6
7	26.6	31.3	39.7	52.2	24.0	26.3	14.5	14.2	13.7

Image Analysis

The MSS spectral bands are not the best for discriminating between the altered and unaltered rocks in the Goldfield mining district, because they are not situated to take full advantage of the distinguishing spectral features (figs. 4a and b). Absence of the 2.2 μm OH-band is especially detrimental, because this feature should be useful for discriminating altered rocks from some unaltered rocks such as the pink tuff discussed above. In addition, the response range of MSS band 7 (0.8-1.1 μm) is broader than the 0.90 μm iron-absorption band so that this feature is weakly expressed in the MSS radiance data. These spectral limitations of the MSS mean that only small spectral radiance differences between altered and unaltered rocks can be recorded; the differences are not evident in the individual MSS images or in color-infrared composites (Rowan and others, 1975a, b).

The subtleness of the MSS spectral differences between the altered and unaltered rocks in the Goldfield district is illustrated by comparing reflectances (Table 2) calculated from the spectra in fig. 4a and b. These values are not representative of the absolute MSS radiances because we did not account for the solar spectrum factor and the MSS system response. However, they are useful for comparative purposes. In each of the MSS bands, the calculated reflectances of the unaltered rocks span the entire range of the altered rocks, emphasizing the limited value of albedo for discriminating these rocks. Some of the band to band differences are reasonably large and diagnostic but others are small and, taken individually, not distinctive. For example, the band 4 to band 5 reflectance difference for hematitic silicified rocks is considerably larger than those for the unaltered rocks because of the intense absorption bands typical of hematite. In contrast, the band 5 to band 6 differences for montmorillonitic argillized rocks and for tuff are small and would be easily obscured by brightness variations due to small changes in topographic slope. Digital computer processing is required for enhancing such subtle spectral radiance differences.

Several techniques have been used for displayirg the subtle MSS radiance differences which appear to typify altered and unaltered areas, including digital classification (Schmidt, 1975; Schmidt and others, 1975) and simulated true color (Albert, 1975), but the most effective approach in the south-central Nevada study area (fig. 1) involves interpretation of color composites of ratio images (Rowan and others, 1974). Ratios of spectral band images are useful for several reasons: (1) the differences between slopes of reflectance spectra between two bands can be displayed in a single image; (2) to first order, brightness variations caused by variations in topographic slope attitude are removed and the responses from like materials are normalized; (3) the response of the members of a like class of materials having similar reflectance curve shapes but varying albedos are normalized; and (4) the width of the distribution of image brightness values is reduced so that a greater contrast stretch can be applied.

Figure 5 illustrates the varying illumination conditions. A simplified expression for the brightness perceived at the spacecraft is given by

$$K_x = G_x \rho_x \Phi + N_x \qquad (1)$$

where the subscript x denotes the wavelength band, G is a system factor containing the instrument response, atmospheric transmittance and solar irradiance, ρ is the bidirectional spectral reflectance, Φ is the photometric function given in 2, and N is the path radiance or contribution from the scattered light in the intervening atmosphere. Assuming a lambert surface and ignoring a small wavelength dependence, then

$$\Phi = \cos \alpha \qquad (2)$$

where $\cos \alpha = \cos s \cos \gamma + \sin s \sin \gamma \cos \theta$ and s is the angle between z and the vertical, θ is the azimuth angle between the slope and the sun.

Figure 5 and 6 near here

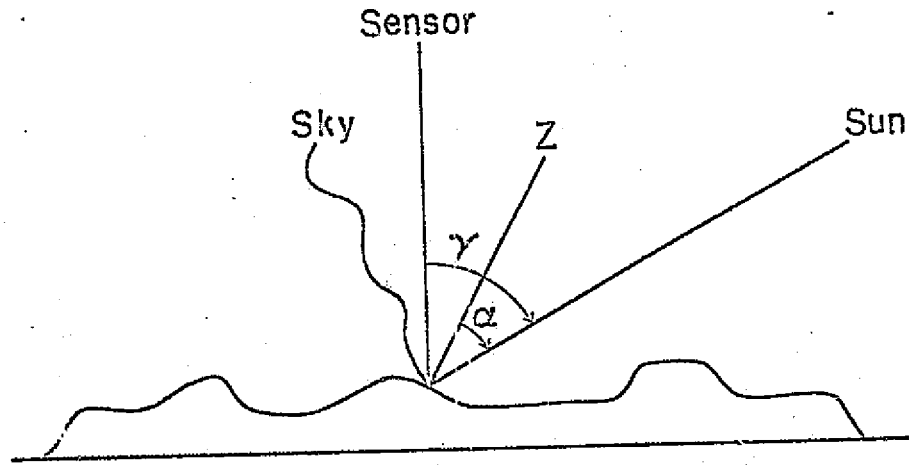
Sensor
Sky
Z
Sun
γ
α

Figure 5 - Simplified two dimensional radiation geometry diagram. α is the angle between the surface normal (Z) and the sun, γ is the solar zenith angle.

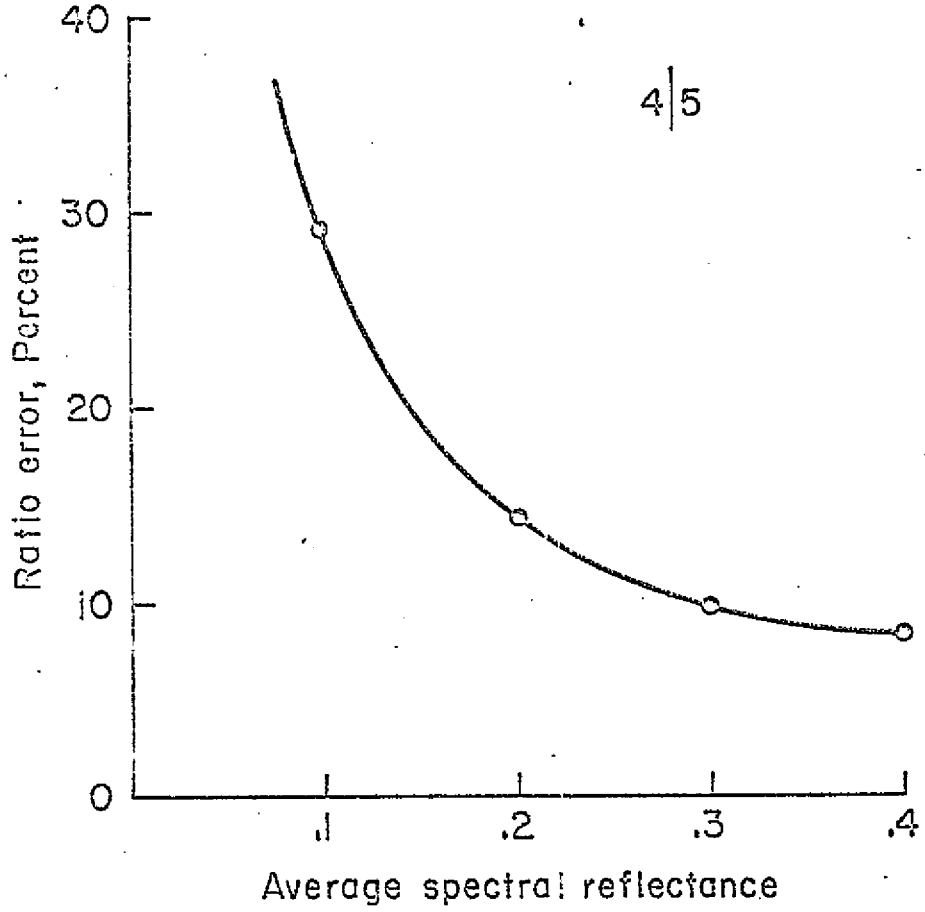
40
30
20
10
0
Ratio error, Percent
.1
.2
.3
.4
Average spectral reflectance

Figure 6 - Error introduced in the ratio as a function of average spectral reflectance if the path radiance correction is not made. The values were calculated for a ratio of MSS bands 4/5 using atmospheric values as given by Goetz et al (1975).

Ratioing two spectral bands yields the expression

$$\frac{K_1}{K_2} = \frac{G_1\rho_1}{G_2\rho_2}\left(1 - \frac{N_2}{G_2\rho_2\Phi}\right) + \frac{N_1}{G_2\rho_2\Phi}\left(1 - \frac{N_2}{G_2\rho_2\Phi}\right) + \ldots \qquad (3)$$

The first order term $\frac{G_1\rho_1}{G_2\rho_2}$ is now independent of the slope of the surface except that sky illumination (not represented here) will become a significant factor for large absolute values of α in fig. 5. If the additive terms are first removed, then the cross products in equation 3 disappear. The path radiance term can be estimated by determining the values for deep, clear water bodies in the scene or using cloud shadows, as outlined by Goetz et al. (1975), or by determining the value of the additive term which yields the lowest variance in the ratio values in the scene (Soderblom, private communication).

Figure 6 shows the error induced in the ratio if the scene is not corrected for path radiance. Although this error is substantial, the correction destroys an undesirably large amount of spatial information. Therefore, no path radiance correction was applied to the ratio images discussed in the following section. In practice, this error has the effect of reintroducing albedo and slope information into the ratio image, but the effect is less disturbing to the analyst than severe loss of spatial detail. However, if quantitative values are desired, a path radiance correction must be made before the ratio is taken. Sky illumination of slopes at high angles of α cannot be corrected for without a detailed knowledge of the topography. For this reason, lithologic mapping is best done with high sun angle images.

Selection of the optimum ratio image or combination of images can be determined by evaluating ratios calculated from spectra representing the rock units of interest (Table 3). Some units can be distinguished in a single ratio image. For example, MSS 4/5 or the inverse, MSS 5/4, images are recognized as being especially useful for detecting iron-oxide-rich zones (Vincent, 1975; Short and Maars, 1975). Low MSS 4/5, MSS 4/6, and MSS 4/7 ratios are related to the intense ferric-absorption band in the hematite spectrum. However, some rocks such as the montmorillonitic argillized rocks and basalt (Table 3), have small MSS 4/5 differences and therefore, a composite of two or more ratio images is needed for discriminating among them. The spectral information discussed here was not available when various color-ratio composites were being prepared and evaluated for the study area. Consequently, a time-consuming trial and error process was necessary for selecting the best combination of ratio images and diazo colors.

The color-ratio composite found most useful for discriminating between altered and unaltered rocks, as well as among the unaltered rocks, in the initial study area in south-central Nevada (fig. 1) is composed of the following stretched-ratio image combinations using diazo color: blue for MSS 4/5, yellow for MSS 5/6, and magenta for MSS 6/7. In this composite, basaltic and intermediate rocks are white, felsic rocks are pink to light orange, and altered rocks are green to dark green and brown to red-brown (fig. 7). These colors are essentially the same as described by Rowan and others (1974) for the initial composite of the eastern part of this scene except that all the colors are more intense. This change was accomplished by using two yellow separates for MSS 5/6 and slightly more complete developing for the separates than was used in preparing the initial composite. The more intense colors facilitate interpretation of the color-ratio composite.

Figure 7 near here

Table 3

MSS ratios for altered and untered rocks in the Goldfield, Nevada mining district calculated from the reflectance values in Table 2.

	Altered Rocks			Unaltered Rocks					
MSS bands	Hematitic silicified	Hematitic argillic silicified	Montmorillonitic argillized	Playa deposits	Tuff	Latite	Rhyodacite	Trachyandesite	Basalt
4/5	.58	.79	.81	.96	.83	.89	.88	.86	.83
5/6	.87	.90	1.00	.98	.89	.98	.95	.99	.90
6/7	.99	.93	1.07	1.00	.91	1.00	.99	1.05	.91
4/6	.51	.71	.81	.94	.73	.87	.83	.85	.75
5/7	.87	.83	1.07	.98	.81	.98	.94	1.04	.82
4/7	.51	.66	.87	.94	.67	.87	.82	.89	.69

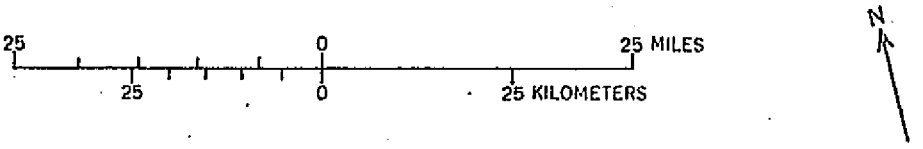

Figure 7. Color ratio composite of MSS scene E1072-18001 consisting of the following stretched ratio image combinations using diazo colors: blue for MSS 4/5, yellow for MSS 5/6, and magenta for MSS 6/7. Basaltic and intermediate volcanic rocks and black shale appear white, felsic rocks are pink to red, playas are blue, vegetation is orange, and altered rocks are green to dark green and brown to red-brown. A, alluvial areas; B, tan shale; C, red shale; D, Pink tuff; E, altered tuffs in the Ralston mining district; F, altered tuffs along west flank of Stonewall Mountain; G, unaltered tuff near Tolicha Peak; and H, unaltered tuff west and south of Montezuma Peak. Image recorded on October 3, 1972.

Evaluation of the initial color-ratio composite of the eastern part of the study area (fig. 1) showed that alluvial areas are commonly represented by various tints of green and brown in the image (A, fig. 7), similar to the colors representing hydrothermally altered rocks. In some places, the alluvium was derived from altered rocks, but in others iron oxide has formed on the surfaces of fragments derived from unaltered rocks. The first steps required for preparing an alteration map from the color-ratio composite, therefore, is distinguishing outcrop from alluvial areas. This process is significantly aided by photointerpretation of Skylab color photographs (fig. 8), but can be achieved using contrast-stretched MSS images (see Rowan and others, 1974, fig. 14).

Agreement between the green to dark green and brown to red-brown areas and hydrothermally altered outcrops was found to be excellent in the eastern part of the study area (fig. 1) (Rowan and others, 1974). Only two areas portrayed in these colors are unaltered rocks, and all of the known altered areas were detected. Continued evaluation of the initial color-ratio composite image and evaluation of the new composite showing the entire scene (fig. 7) have reaffirmed these generally positive conclusions. However, analysis of the western part of the composite (fig. 7) shows that several unaltered rocks are displayed in colors similar to those of the altered rocks. One of the main objectives of this study is to determine the limitations of this approach for mapping hydrothermal alteration zones. Therefore, the remainder of this paper deals with these problematical rock types.

As previously described, tan and red shales and bright pink tuff in the western part of the study area (A, B, and C, respectively, fig. 8) are spectrally similar to altered rocks (figs. 3 and 4a) in the MSS response range. Therefore, these rocks appear green in the color-ratio composite (B, C, and D, respectively, fig. 7), although they are unaltered. It is important to point out that slightly pink, tan, and gray silicic tuffs and flows are common in the study area, but are consistently pink to orange-pink in the color-ratio composite (fig. 7). Tan to brown siltstone and shale constitute one of the problematical rocks discussed by Rowan and others (1974) in the eastern part of the area. Although spectra are not available for this rock type, they are undoubtedly similar to those for the tan and red shales and the altered rocks. The other problematical rock type in the eastern part is an intrusive of generally andesitic composition (see K, fig. 17, Rowan and others, 1974); spectral measurements are not available for this area.

Figure 8 near here

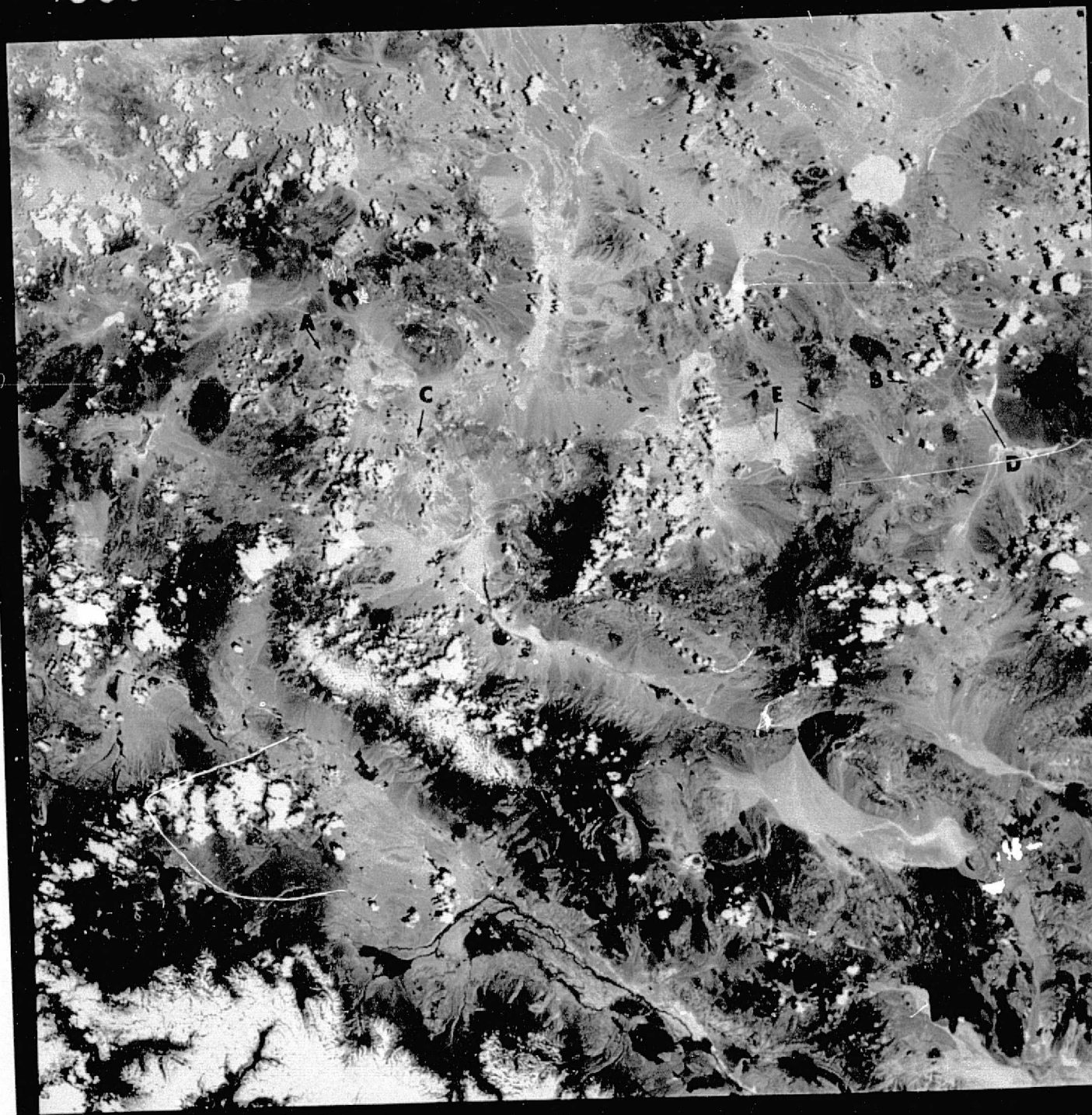

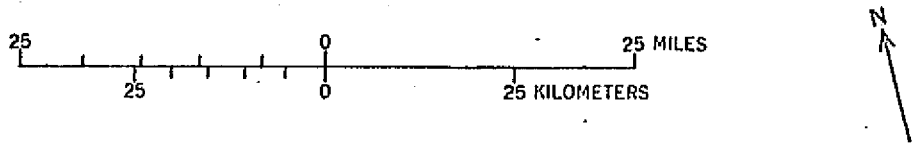

Figure 8. Skylab S190A color photograph of part of the study area. A, tan shale; B, red shale; C, pink tuff; D, altered tuff in the Ralston mining district; and E, unaltered tuff west and south of Montezuma Peak. Photographed 3 June 1973. Ektachrome film, type SO 356.

In addition, rocks appearing red-brown in the color-ratio composite (fig. 7) are problematical because, although some consist of altered rocks, others appear to be unaltered. For example, tuffs in the Ralston mining district (E, fig. 7 and D, fig. 8) and along the west flank of Stonewall Mountain (F, fig. 7) have been altered to very fine-grained, locally opaline silica, but two areas near Tolicha Peak (G, fig. 7) and large areas west and south of Montezuma Peak (H, fig. 7 and E, fig. 8) consist of glassy tuff without any obvious hydrothermal alteration. All these rocks are rhyolitic tuff, which have very high albedos. Iron-oxide minerals are generally absent or minor, indicating that little iron sulphide was introduced during the epithermal silicification process that affected some of these areas. Thus, these rocks are portrayed in the color-ratio composite in a color that differs only slightly from that of other silicic tuffs and flows, and the iron-poor silicified tuffs and flows and their apparent unaltered equivalents are not consistently discriminable in the composite.

In spite of these problems, as estimated 80 percent of the green to dark green and brown to red-brown areas in the color-ratio composite are related to hydrothermal alteration. However, these results do emphasize the dependence of this technique on the presence of contrasting ferric-iron oxide absorption intensities between altered and unaltered rocks and the necessity for supplementary information where this contrast is lacking. In MSS color-ratio composites, unaltered rocks rich in iron-oxide minerals stains will appear altered, and altered rocks poor in iron-oxides will appear unaltered. The most promising spectral region for solving some of these problems appears to be near 2.2 μm. In this region, unaltered rocks with strong iron absorption band, but low hydroxyl content, such as the pink tuff of the northern Silver Peak Range, should be discriminable from hydrothermally altered rocks on the basis of the absence of the 2.2 μm band in the spectra for these unaltered rocks. More importantly, hydrothermally altered rocks should be distinguishable in this spectral region independent of their ferric iron content because of the presence of the 2.2 μm band in their spectra.

Conclusions

In the MSS response range, the spectral reflectance differences between the altered and unaltered rocks in the Goldfield mining district are due to the increased abundance of hematite, goethite, jarosite, and montmorillonite in the altered rocks. This mineral assemblage results in intense iron-absorption bands in the 0.45-1.1 μm part of the *in situ* reflectance spectra for most of the altered rocks; these spectral features are absent or weakly expressed in most of the unaltered rock spectra. Although the MSS bands are not optimum for detecting these spectral differences, approximately 80 percent of the areas displayed as green and brown in a color-ratio composite of the study area were found to be related to hydrothermal alteration. Therefore, detection of mineralogically similar alteration zones in other well exposed regions should be possible using this approach.

However, some unaltered rocks, such as the pink hematitic tuff and tan and red shales are spectrally similar to the altered rocks in the MSS bands. Judging from the field spectra obtained thus far, the 2.2 μm region is promising for resolving some of these problems because the OH combination overtone band that typifies the altered rocks at Goldfield is absent in most of the unaltered rock spectra. Furthermore, the Goldfield altered rocks represent only one type of alteration where the mineral assemblages cause intense iron-absorption bands. Some unaltered areas, such as the silicified tuffs near Tolicha Peak and Montezuma Peak lack distinctive iron-absorption bands; they are characterized by an intense 2.2 μm OH absorption band, however. Detection of these and spectrally similar altered areas in satellite and aircraft images may require a band centered near 2.2 μm.

References Cited

Albers, J. P. and Kleinhampl, F. J., 1970, Spatial relation of mineral deposits to Tertiary volcanic centers in Nevada: U. S. Geol. Survey Prof. Paper 700-C, p. C1-C10.

Albers, J. P. and Stewart, J. H., 1972, Geology and mineral deposits of Esmeralda County, Nevada: Nevada Bur. Mines and Geol. Bull. 78, 80 p.

Albert, Nairn, R. D., 1975, Interpretation of Earth Resources Technology Satellite imagery of the Nabesna quadrangle, Alaska: U. S. Geol. Survey Misc. Field Studies Map MF-655-J, sheets 1 and 2, scale 1:250,000.

Ashley, R. P., 1970, Evaluation of color and color infrared photography from the Goldfield mining district, Esmeralda and Nye Counties, Nevada: U. S. Geol. Survey open-file report, 36 p.

_____, 1971, Preliminary geologic map of the Goldfield mining district Nevada: U. S. Geol. Survey open file map, 1 sheet.

_____, 1974, Goldfield mining district, in Guidebook to the geology of four tertiary volcanic centers in central Nevada: Nevada Bur. Mines and Geol. Report 19, pp. 49-66.

Ashley, R. P. and Keith, W. J., 1973, Geochemistry of the altered area at Goldfield, Nevada including anomalous and background values for gold and ore metals: U. S. Geol. Survey open-file report, 117 p.

Ashley, R. P. and Albers, J. P., 1975, Distribution of gold and other ore-related elements near ore bodies in the oxidized zone at Goldfield, Nevada: U. S. Geol. Survey Prof. Paper 843-A, 48 p.

Cornwall, H. R., 1972, Geology and mineral deposits of southern Nye County, Nevada: Nevada Bur. Mines and Geol. Bull. 77, 45 p.

Goetz, A. F. H., Billingsley, F. C., Gillespie, A. R., Abrams, M. J., Squires, R. L., Shoemaker, E. M., Lucchitta, I., and Elston, D. P., 1975, Application of ERTS images and image processing to regional geologic problems and geologic mapping in Northern Arizona: Jet Propulsion Laboratory Tech. Report 32-1597, 188 p., Pasadena, Calif.

Harvey, R. D. and Vitaliano, C. J., 1964, Wall-rock alteration in the Goldfield district, Nevada: Jour. Geology, v. 72, p. 564-579.

Hunt, G. R. and Salisbury, J. W., 1970, Visible and near infrared spectra of minerals and rocks-I. Silicate minerals: Modern Geology, v. 1, no. 4, p. 238-300.

Hunt, G. R., Salisbury, J. W., Lenhoff, C. J., 1971, Visible and near infrared spectra of minerals and rocks-IV. Supphides and sulphates: Modern Geology, v. 8, no. 1, p. 1-14.

____, 1973, Visible and near infrared spectra of minerals and rocks-IV. Additional silicates: Modern Geology, v. 4, p. 85-106.

Jensen, M. L., Ashley, R. P., and Albers, J. P., 1971, Primary and secondary sulphates at Goldfield, Nevada: Econ. Geology, v. 66, p. 618-626.

Locke, Augustus, 1912a, The ore deposits of Goldfield-I: Eng. and Mining Jour., v. 94, p. 797-802.

_____, 1912b, The ore deposits of Goldfield-II: Eng. and Mining Jour., v. 94, no. 18, p. 843-849.

Ransome, F. L., 1909, Geology and ore deposits of Goldfield, Nevada: U. S. Geol. Survey Prof. Paper 66, 258 p.

_____, 1910a, Geology and ore deposits of the Goldfield district, Nevada. Part I-Geology: Econ. Geology, v. 5, no. 4, p. 301-311.

_____, 1910b, Geology and ore deposits of the Goldfield district, Nevada. Part II-Mines and mining: Econ. Geology, v. 5, no. 5, p. 438-470.

Rowan, Lawrence C., Wetlaufer, Pamela H., Billingsley, F. C., and Goetz, Alexander F. H., 1973, Mapping of hydrothermal alteration zones and regional rock types using computer-enhanced ERTS MSS images, in Third ERTS Symposium, Abstracts, Dec. 10-14, 1973, Washington, D. C., paper no. G16, p. 52.

Rowan, Lawrence C., Wetlaufer, Pamela H., Goetz, Alexander F. H., Billingsley, Fred C., and Stewart, John H., 1974, Discrimination of rock types and detection of hydrothermally altered areas in south-central Nevada by use of computer-enhanced ERTS images: U. S. Geol. Survey Prof. Paper 883, 35 p.

Rowan, Lawrence C. and Wetlaufer, Pamela H., 1975a, Iron absorption band analysis for the discrimination of iron-rich zones: NASA Type III report, 160 p.

Rowan, Lawrence C., Goetz, Alexander, F. H., Ashley, Roger P., 1975b, Use of spectral reflectance measurements of altered and unaltered rocks in south-central Nevada as a basis for enhancement of Landsat images, in NASA Earth Resources Survey Symposium, Abstracts, June 8-13, 1975, Houston, Tx, paper no. G-6, p. 113-114.

Searls, Fred, Jr., 1948, A contribution to the published information on the geology and ore deposits of Goldfield, Nevada: Nevada Univ. Bull., v. 42, no. 5 (Geology and Mining Ser. no. 48), 24 p.

Schmidt, Robert G., 1975, Exploration for porphyry copper deposits in Pakistan using digital processing of ERTS-1 data: U. S. Geol. Survey open file report, 29 p.

Schmidt, R. G., Clark, B. B., Bernstein, R., 1975, A search for sulphide-bearing areas using Landsat-1 data and digital image-processing techniques, in NASA Earth Resources Survey Symposium, Abstracts, June 8-13, 1975, Houston, Tx, paper no. G-26, p. 150-151.

Short, Nicholas M. and Maars, Ronald W., 1975, The anatomy of an anomaly, in NASA Earth Resources Survey Symposium, Abstracts, June 8-13, 1975, Houston, Tx, paper no. G-5, p. 110-112.

Vincent, Robert K., 1975, Oil, gas exploration tool - composite mapping of earth from satellite information: Oil and Gas Journal, Feb 17, 1975, p. 141-142.